Modelling Thermomechanical Response of a Diamond Particle in a Metallic Matrix

Jan LACHOWSKI[1], Joanna BOROWIECKA-JAMROZEK[2]

Kielce University of Technology
[1] *Faculty of Management and Computer Modelling*
[2] *Faculty of Mechatronics and Mechanical Engineering*
Al. Tysiąclecia Państwa Polskiego 7, 25-314 Kielce, Poland
e-mail: jlach@tu.kielce.pl

The paper deals with numerical and analytical modelling of synthetic diamond particle retention in a metallic matrix. The model of a diamond particle embedded in a metallic matrix was created using the Abaqus software. The numerical results were compared with the experimental data. The analytical model of a spherical particle in a metallic matrix was built. The analysis has indicated the mechanical parameters responsible for the retention of diamond particles in a matrix.

Key words: synthetic diamond, metallic matrix, finite element method.

1. Introduction

Circular saws containing diamond-metal segments are used for cutting construction materials and natural stones (Fig. 1) [1, 2]. Segments are working elements of a saw blade produced by means of the powder metallurgy technology. A significant feature of a segment metallic matrix is diamond particle retention during the operation of a diamond impregnated tool. Diamond particles are retained in the matrix by mechanical bonding [2]. The bonding is obtained during cooling after the hot pressing process. Compared with metals, diamond has a very low coefficient of thermal expansion, and therefore diamond particles are tightened by the contracting matrix. Proper mechanical bonding depends on elastic and plastic properties of the matrix.

Depending on synthesis conditions, diamond crystallization results in different shapes ranging from a cube to an octahedron (Fig. 2) [2]. The truncated octahedron, the size of which was determined by the distance of 350 μm between the opposite square facets, was selected for the 3D numerical analysis (Fig. 2).
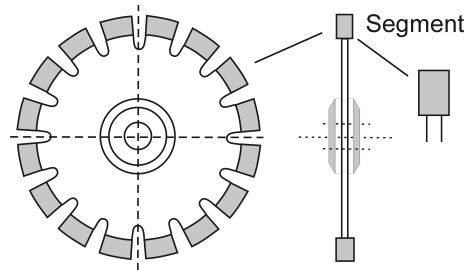
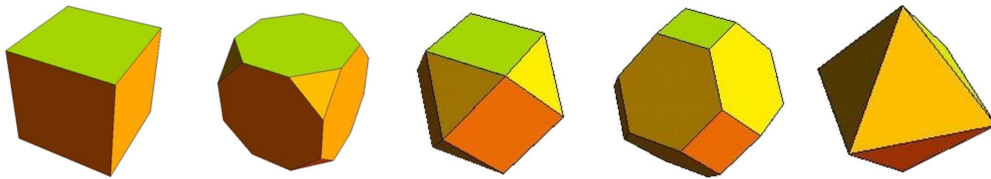FIG. 1. Schematic representation of a circular saw blade.

FIG. 2. Typical shapes of a synthetic diamond crystal: cube, truncated cube, cuboctahedron, truncated octahedron, octahedron.

2. ANALYSIS OF DIAMOND PARTICLES RETENTION IN A METALLIC MATRIX

2.1. Numerical analysis

The computer modelling was carried out using the finite element method and the ABAQUS Ver. 6.14 software. The 3D computer model was created for a diamond crystal embedded in the cobalt matrix (Fig. 3a) [3] and a diamond crystal protruding 50 μm above the matrix surface (Fig. 3b). The boundary conditions were as follows: the displacement Y was fixed at the front of the model and the displacement X was fixed at the bottom of the model.
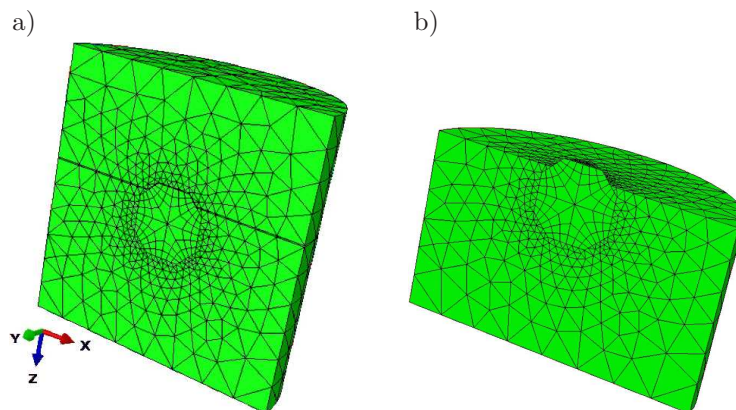

FIG. 3. Model of a diamond crystal: a) inside the matrix, b) protruding above the matrix surface.

The problem was analyzed by performing simulations for the model of the diamond particle and two layers of the matrix (Fig. 3a). Initially, the particle was placed inside the matrix during the simulation of the hot pressing process. The simulation was conducted by applying the maximum pressure and the maximum temperature. The temperature was then reduced to the ambient temperature and the pressure was removed.

Subsequently, the upper layer of the matrix was removed and the particle was exposed to the predetermined value of protrusion. It simulates uncovering of the particle during a diamond tool operation. The diamond particle retention at the surface can be assessed by performing a simulation of the particle pull-out by an external force [4].

The temperature and the pressure applied during the hot pressing process were assumed to be 850°C and 35 MPa. The mechanical parameters of diamond and cobalt are typical values employed in the analysis of metal-bonded diamond composites [3]. The average values of the coefficient of thermal expansion for diamond and the metal matrix were $3 \cdot 10^{-6}$ K^{-1} and $14 \cdot 10^{-6}$ K^{-1}, respectively.

The simulation results for the diamond particle protruding above the matrix surface (Fig. 3b) were compared with the experimental data. There is only one experiment that can be used to determine stresses inside a diamond crystal in a cobalt matrix. The technique of Raman spectroscopy was employed to measure the pressure in the particle at the surface of a cobalt matrix [5]. The pressure was measured along the diamond symmetry axis from the top crystal facet to the bottom facet (Fig. 3b). Figure 4 compares the numerical results with the experimental data of two diamond crystals. The numerical results are in agreement with the experimental curve; the shape and the maximum values are close together (Fig. 4).
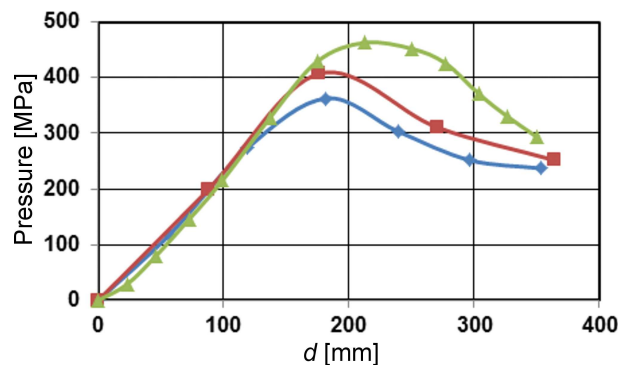

Fig. 4. Comparison of computer simulations results with the experiment [4], the simulation results – blue plot, the experimental data – green and red plots, d is the distance from the top facet (Fig. 3b).

2.2. Mathematical model of a diamond particle in an elastic-plastic matrix

In the case of spherical symmetry and in the absence of body forces, the following equilibrium equation for the continuum is given [6]:

$$(2.1) \qquad \frac{d}{dr}\left(\frac{1}{r^2}\frac{d\left(r^2 u_r\right)}{dr}\right) = 0,$$

where r is a radial coordinate in the spherical coordinate system with the origin in the particle centre.

There are the following boundary conditions resulting from the model of the particle in the matrix (Fig. 5a): displacements at the particle centre ($r = 0$) and displacements in the matrix at infinity ($r = \infty$) are equal to zero, $u_r = 0$. Thus, the solution of the Eq. (2.1) for the particle is given by:

$$(2.2)_1 \qquad u_r = -ar$$

and for the matrix:

$$(2.2)_2 \qquad u_r = \frac{b}{r^2},$$

where the constants of integration a and b are positive. Radial displacements $(2.2)_1$ and $(2.2)_2$ at the particle-matrix border must follow compatibility conditions of displacements:

$$(2.3) \qquad aR + \frac{b}{R^2} = R\left(\alpha_M - \alpha_D\right)\Delta T,$$

where α_M and α_D are coefficients of thermal expansion for the matrix and the particle respectively, and ΔT is the temperature difference during cooling after the hot pressing (Fig. 5a).
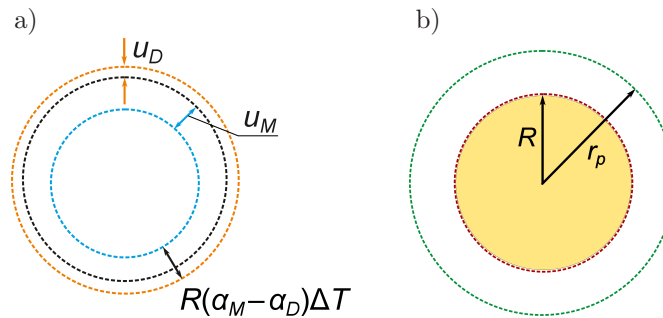

Fig. 5. Model of the particle in the matrix: a) displacements at the particle-matrix border, b) the plastic zone around the particle.

Radial and circumferential strains are calculated by the following expressions [6]

$$(2.4) \qquad \varepsilon_{rr} = \frac{\partial u_r}{\partial r}, \qquad \varepsilon_{\theta\theta} = \varepsilon_{\varphi\varphi} = \frac{u_r}{r}.$$

In the spherical coordinate system, in the elastic regions ($r < R$ and $r > r_p$ in Fig. 5b), the Hooke's Law is expresses by [6]:

$$(2.5) \quad \sigma_{rr} = \frac{E}{(1+\nu)} \left(\varepsilon_{rr} + \frac{\nu}{1-2\nu} e \right), \qquad \sigma_{\varphi\varphi} = \frac{E}{(1+\nu)} \left(\varepsilon_{\varphi\varphi} + \frac{\nu}{1-2\nu} e \right),$$

where E is the elastic modulus, ν denotes the Poisson's ratio, and e is the first invariant of strain tensor. Introducing the displacements (2.2) into (2.4), and then into (2.5), stress components in the diamond particle are obtained

$$(2.6) \qquad \sigma_{rr} = \sigma_{\varphi\varphi} = -\frac{E_D}{(1-2\nu_D)} a,$$

as well as radial and circumferential stress in the metallic matrix

$$(2.7) \qquad \sigma_{rr} = -\frac{2E_M}{1+\nu_M} \frac{b}{r^3}, \qquad \sigma_{\varphi\varphi} = \frac{E_M}{1+\nu_M} \frac{b}{r^3}.$$

The following relationship between a and b constants is given by the continuity of radial stress at the matrix-particle border:

$$(2.8) \qquad -\frac{E_D}{1-2\nu_D} a = -\frac{2E_M}{1+\nu_M} \frac{b}{R^3},$$

where R is the diamond particle radius. The a and b constants are defined by the system of Eqs. (2.3) and (2.8).

The above formulas are valid for an elastic range. The plastic zone around the particle is formed with the sufficiently high temperature difference (Fig. 6).
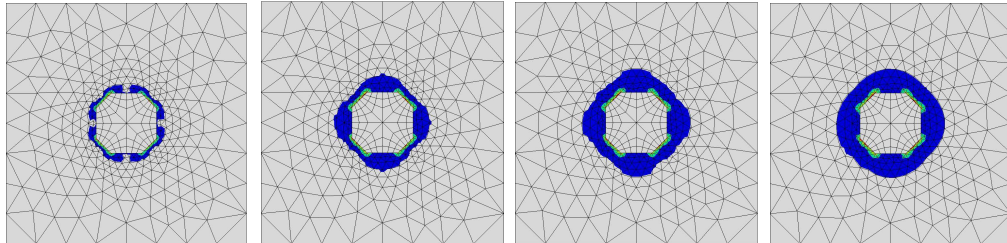

FIG. 6. The formation of the plastic zone around the particle during cooling (from left to right).

Radial stress in the plastic zone ($R < r < r_p$ in Fig. 5b) is given by [8]

$$(2.9) \qquad \sigma_{rr} = -2\sigma_0 \ln\left(\frac{r_p}{r}\right) - \frac{2}{3}\sigma_0,$$

where r_p is the radius of plastic zone and σ_0 is the yield stress. Since the displacement at the matrix border can be denoted by u_M (Fig. 5a), stress in the particle can be calculated from $(2.2)_2$, (2.3) and (2.6):

$$(2.10) \qquad \sigma_{rr} = \frac{E_D}{1 - 2\nu_D}\left(R\left(\alpha_M - \alpha_D\right)\Delta T - \frac{u_M}{R}\right).$$

The displacement of the matrix border as the function of the plastic zone radius was obtained in model [7]

$$(2.11) \qquad \frac{u_M}{R} = \frac{\sigma_0}{E_M}\left(1 - \nu_M\right)\frac{r_p^3}{R^3} - \frac{2\left(1 - 2\nu_M\right)}{3}\frac{\sigma_0}{E_M}\left(3\ln\left(\frac{r_p}{R}\right) + 1\right).$$

Introducing the formula (2.11) into (2.10), comparing (2.9) with (2.10), and subsequently transforming, the following equation for the plastic zone radius is provided:

$$(2.12) \quad \left(1 - \nu_M\right)\frac{r_p^3}{R^3} - 2\left(\left(1 - 2\nu_M\right) - \left(1 - 2\nu_D\right)\frac{E_M}{E_D}\right)\left(\ln\left(\frac{r_p}{R}\right) + \frac{1}{3}\right)$$
$$= \frac{E_M}{\sigma_0}\left(\alpha_M - \alpha_D\right)\Delta T.$$

The plastic zone radius can be calculated numerically from (2.12). The pressure in the particle is calculated immediately from (2.9):

$$(2.13) \qquad p_D = 2\sigma_0 \ln\left(\frac{r_p}{R}\right) + \frac{2}{3}\sigma_0.$$

Inside the spherical particle, the stress is constant (formulas (2.6) and (2.13)). On the contrary, the stress (2.7) (the elastic region outside the plastic zone, $r > r_p$) decreases as $1/r^3$. The same functional relations for the inclusion are presented in Mura's monograph [9, formulas (11.44) and (11.45)].

2.3. Results

In order to verify the mathematical model, the analytical calculation results were compared with the simulation results in the 3D numerical model. The calculations were performed for two sinters: cobalt SMS sinter and a sinter from a commercial matrix powder, here referred to as CMP [10]. The CMP powder contained the following basic elements: Fe, Cu, Sn and Zn. The compared results in Table 1 indicate a satisfactory agreement.

Table 1. Comparison of computer simulations results with analytical model results.

Material	Co(SMS)	Co(SMS)	CMP	CMP
Parameter	3D model	Analytical model	3D model	Analytical model
Pressure in particle [MPa]	1048	1141	876	880
Radius of plastic zone (divided by R)	2.10	1.95	1.90	1.81
Elastic energy of particle [mJ]	0.0310	0.0342	0.0208	0.0199

The numerical analysis for the cube, the truncated octahedron and the octahedron has been obtained in the paper [11]. The quantities present in Table 1 are slightly affected by a crystal shape. Hence, they are regarded as indicators of the mechanical state of a diamond particle in a metal matrix.

Diamond concentration in a matrix is based on a scale in which 100 concentration means 4.4 carats per cm^3, i.e. 25% per volume. Practically, any concentration changes from 10 to 40 [2, p. 38]. The model in Fig. 3 has only one particle with the matrix environment suitable for diamond concentration about 30 (8% of the diamond volume in matrix). The diamond concentration about 30 can be used in cutting sandstone [2, p. 127]. The field of elastic strain among particles is additive. Moreover, in the reality particles are far enough so that the plastic zones around particles do not influence each other. Thus, the statistical analysis of a set of diamond particles can be provided from the model of one particle.

3. Conclusions

The diamond particle located inside the metal matrix can be characterized as follows:

- the pressure inside the particle and the elastic energy of the particle are not essentially dependent on the particle shape,
- the particle is surrounded by the plastic zone with a relatively well defined radius.

The above parameters could be used as the indexes of the diamond particle retention in the metal matrix.

References

1. Konstanty J., *Powder metallurgy diamond tools*, Elsevier, Oxford, pp. 39–64, 2005.

2. Konstanty J., *Cobalt as a matrix in diamond impregnated tools for stone sawing applications*, AGH, Dissertations-Monographs, No 104, Kraków, 2002.

3. Borowiecka-Jamrozek J., Lachowski J., *Numerical modelling of stress/strain field arising in diamond-impregnated cobalt*, Archives of Metallurgy and Materials, **59**(2): 443–446, 2014, doi: 10.2478/amm-2014-0073.

4. Borowiecka-Jamrozek J., Lachowski J., *Simulation of retention of a diamond particle in a matrix of diamond-impregnated tools*, Journal of Japan Society of Powder and Powder Metallurgy, **63**(7): 697–700, 2016, doi: 10.2497/jjspm.63.697.

5. Akyuz D.A., *Interface and microstructure in cobalt-based diamond tools containing chromium*, PhD thesis, Ecole Polytechnique Federale de Lausanne, Lausanne, 105–108, 1999.

6. Landau L.D., Lifszitz E.M., *Theory of elasticity*, Pergamon Press Ltd., Oxford, pp. 20–21, 1975.

7. Parton V.Z., Perlin P.I., *Mathematical methods of the theory of elasticity*, Mir Publishers, Moscow, 206–208, 1984.

8. Hill H., *The mathematical theory of plasticity*, Clarendon Press, Oxford (Publisher: Oxford University Press (first published in Oxford classic series in 1998)), pp. 97–101, 1950, first published 1950.

9. Mura T., *Micromechanics of defects in solids*, Martinus Nijhoff Publishers, The Hague, The Netherlands, pp. 74–75, 1982.

10. Borowiecka-Jamrozek J., Konstanty J., *Microstructure and mechanical properties a new iron-base material used for the fabrication of sintered diamond tools*, Advanced Materials Research, **1052**, 520–523, 2014, doi: 10.4028/www.scientific.net/AMR.1052.520.

11. Borowiecka-Jamrozek J., Lachowski J., *An Analysis of the Retention of a Diamond Particle in a Metallic Matrix after Hot Pressing*, Proceedings of 57th International Scientific Conference "Solidification and Crystallization of Metals 2016", 19–21 September 2016, Kielce-Cedzyna, disk CD, will be published in Archives of Foundry Engineering, **17**(1), 2017.